MAE 560 – Applied Computational Fluid Dynamics

Dr. H.P. Huang

Project – 1

Submitted by:

Aditya Bodke

<u>Statement on Collaboration</u>:

No Collaboration

School for Engineering of Matter Transport & Energy

Task 1(a)

In this task, a cylindrical water heater prototype was modeled, and fluid flow simulation was performed inside the heater to analyze the heat transfer. As shown in Figure 1, the geometry of the model consists of a main cylindrical tank of diameter D = 0.6 m and height H = 0.8 m, and two cylindrical inlet and outlet side pipes of diameter d = 0.06 m and length L = 0.15 m. The locations of the inlet and outlet side pipes from the bottom surface are Z_1 = 0.6 m and Z_2 = 0.2 m respectively. After modeling the geometry, the mesh was generated with an element size of 2.3 cm and selecting the inflation setting to program controlled. The choice of the element size for the mesh was a bit higher to accommodate room for mesh refinement at the bottom region of the main cylinder. In this problem, all the surfaces of the system are thermally insulated except the temperature of the bottom plate of the main cylinder was set to a constant value of T = 55°C. The inlet velocity was set to a constant, v_{in} = 0.06 m/s and the inlet temperature was set to a constant, T_{in} = 20°C.
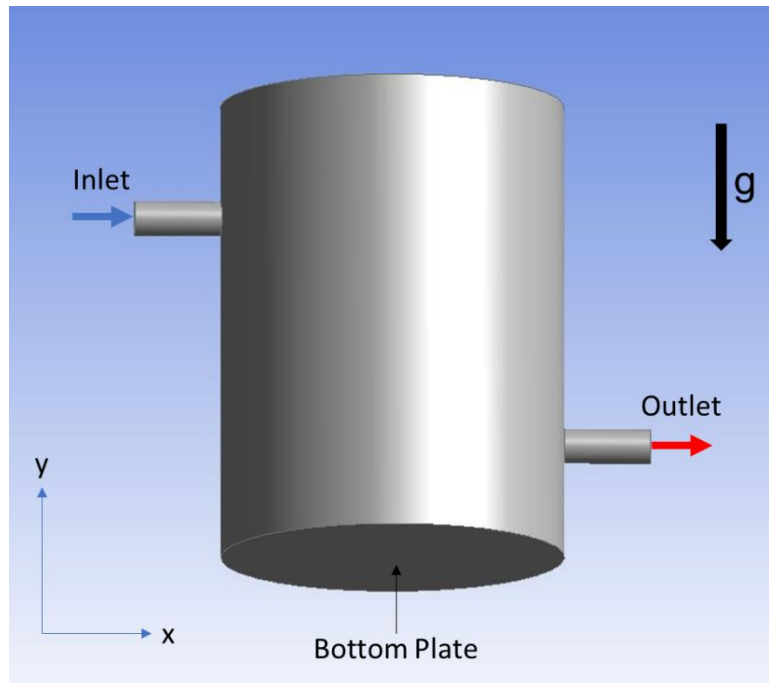

Figure 1. Prototype Water Heater Model

The pressure-based solver was utilized and the gravitational constant in Task 1(a) was considered as g = 9.81 m/s² in the negative y direction. The Boussinesq approximation was applied to the density in order to allow the variation of density with temperature along with the full buoyancy effect selected under the standard k-epsilon turbulence model. The operating temperature, T_o, for the simulation was considered as the average of maximum and minimum values of the temperature in the system, which is computed in Eq. 1:

$$T_o = \frac{T_{max} + T_{min}}{2} = \frac{55\,^oC + 20\,^oC}{2} = 37.5\,^oC = 310.65\ \text{K} \tag{1}$$

The operating density was evaluated based on the formula obtained from the reference NIST paper at the operating temperature value as shown in Eq. 2 below:

$$\rho_o = 999.85308 + 6.32693 \times 10^{-2}T_o - 8.523829 \times 10^{-3}T_o{}^2 \qquad (2)$$
$$+ \; 6.943248 \times 10^{-5}T_o{}^3 - 3.821216 \times 10^{-7}T_o{}^4$$
$$= 993.1448623 \; \frac{kg}{m^3}$$

The thermal expansions coefficient for the system was calculated using Eq. 3:

$$\beta = -\frac{1}{\rho_o}\left(\frac{d\rho}{dT}\right)_{T_o} = 0.00036621 \; \frac{1}{K} \qquad (3)$$

Deliverable (i)

The contour plot of the y-velocity in the plane of symmetry for the steady solution is shown in Figure 2. From the figure, it is evident that the minimum y-velocity is -0.0453 m/s and the maximum y-velocity is 0.0640 m/s. Initially the water enters the inlet pipe and starts to fall downward due to gravity with a negative y-velocity. Later, the water encounters the bottom surface and flows in the x direction. As the water reaches the boundary, it shifts upward with a positive y-velocity and the maximum y-velocity is observed as the water approaches the outlet pipe.
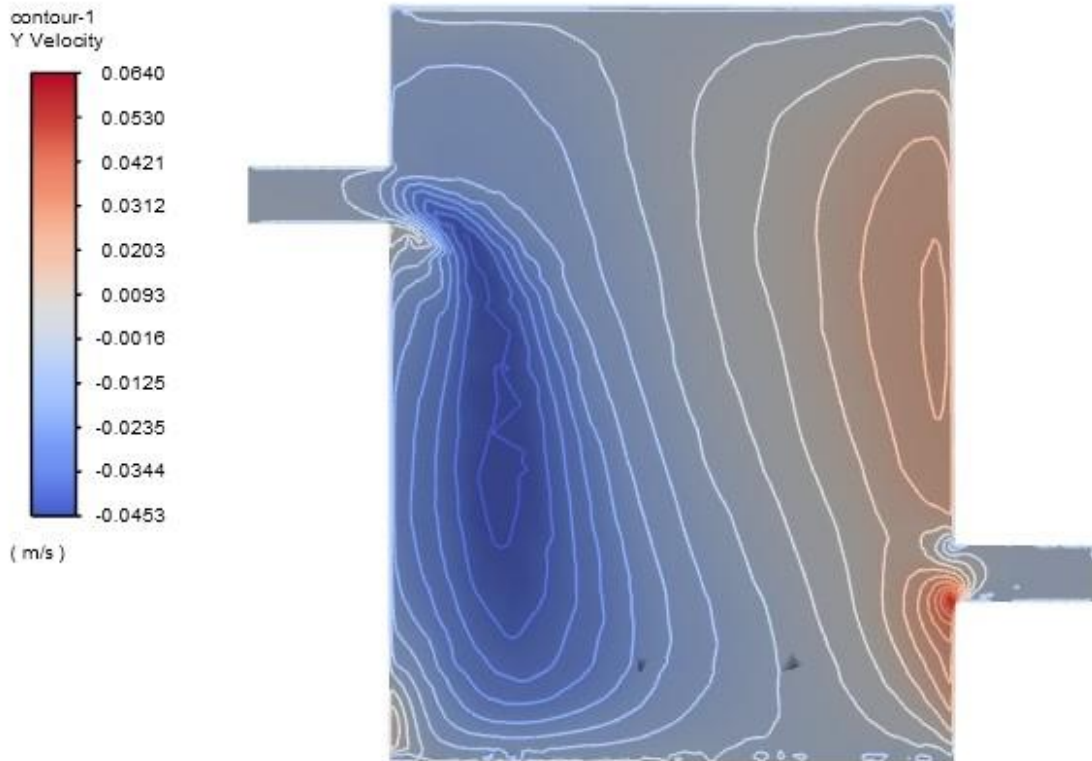

Figure 2. Contour Plot of Y-Velocity in the Plane of Symmetry

Deliverable (ii)

The contour plot of temperature in the plane of symmetry for the steady solution is shown in Figure 3. To clearly highlight the "cool waterfall" coming down from the inlet, the contour interval range of temperatures was manually adjusted between 293 K and 300 K.
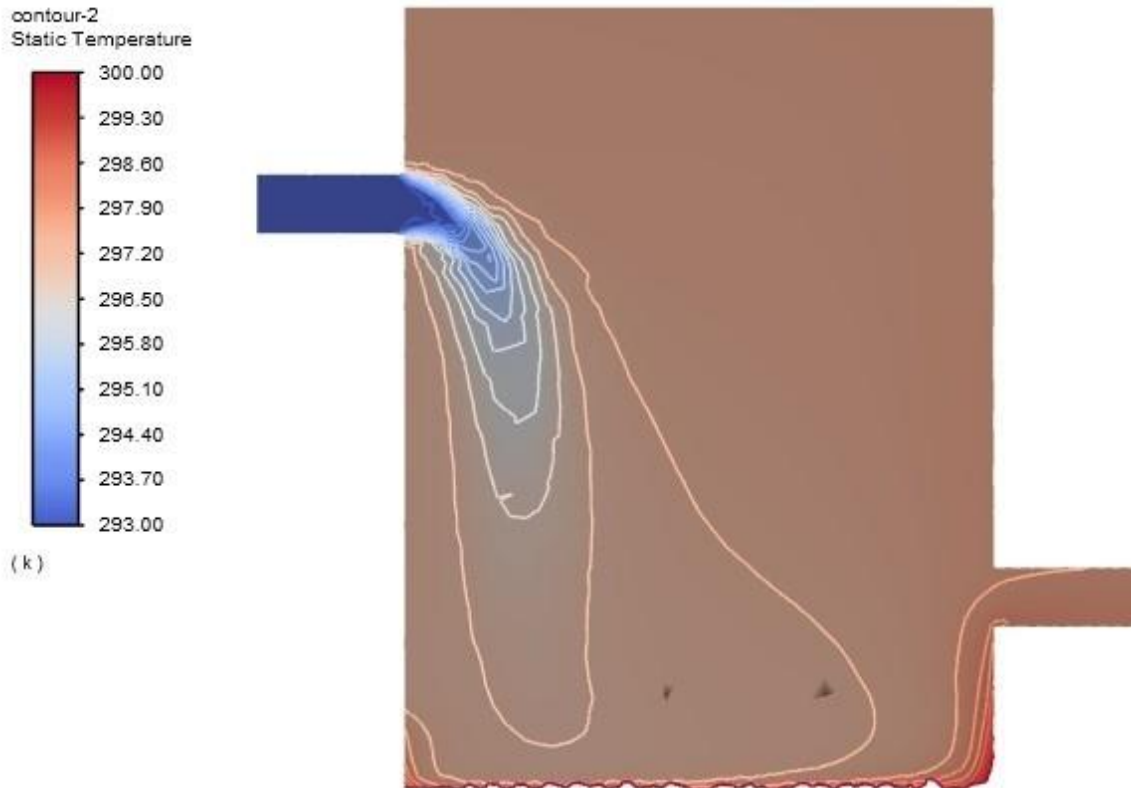

Figure 3. Contour Plot of Temperature in the Plane of Symmetry

Deliverable (iii)

The outlet temperature, T_{out}, is defined as the area-weighted average of static temperature at outlet as shown in Eq. 4:

$$T_{out} = \frac{1}{A} \iint_A T \, dA \tag{4}$$

The value of outlet temperature at the steady state was found to be $T_{out} = 298.01 \, K$.

This value was obtained after running a total of 1500 iterations. Figure 4 depicts the line plot of the outlet temperature, T_{out}, as a function of the number of iterations. The convergence criteria requirement for this task is said to be achieved when the variation of T_{out} is less than 0.1°C over the span of 100 iterations. This was observed between 1000 and 1100 iterations where the

temperature difference achieved was 0.08 K. The simulation was, however, continued until 1500 iterations to achieve the steady value.
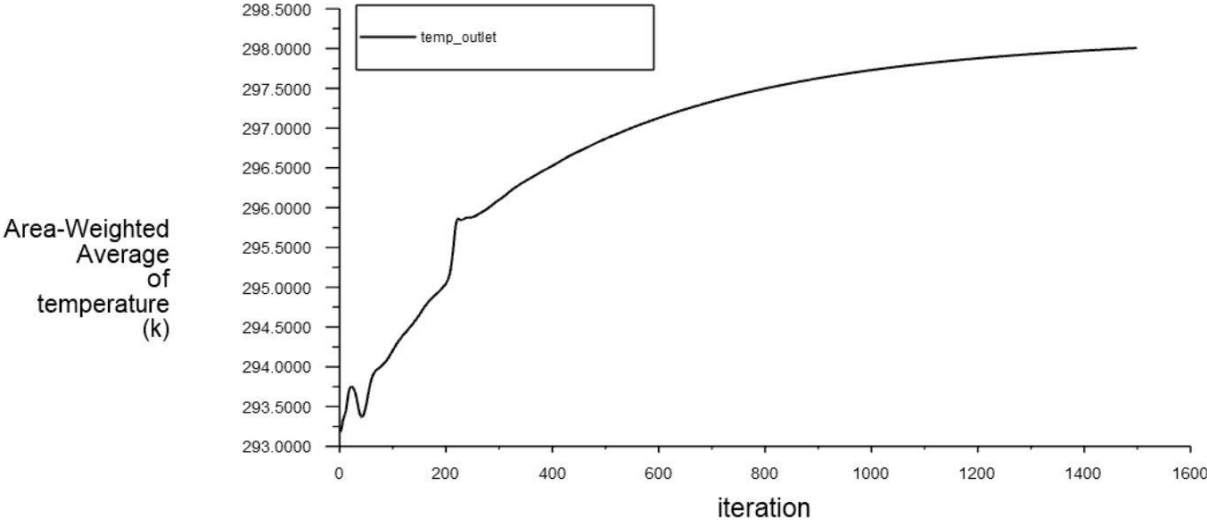

Figure 4. Line Plot of Outlet Temperature vs. Number of Iterations

Deliverable (iv)

A plot of the mesh along the plane of symmetry is shown in Figure 5. The mesh was automatically refined at the boundaries of the main cylinder and inside the inlet and outlet side pipes. Additional mesh refinement was done at the bottom of the main cylinder by defining a pancake region of inner cylinder with a height of 0.1 m and a diameter of 0.6 m.
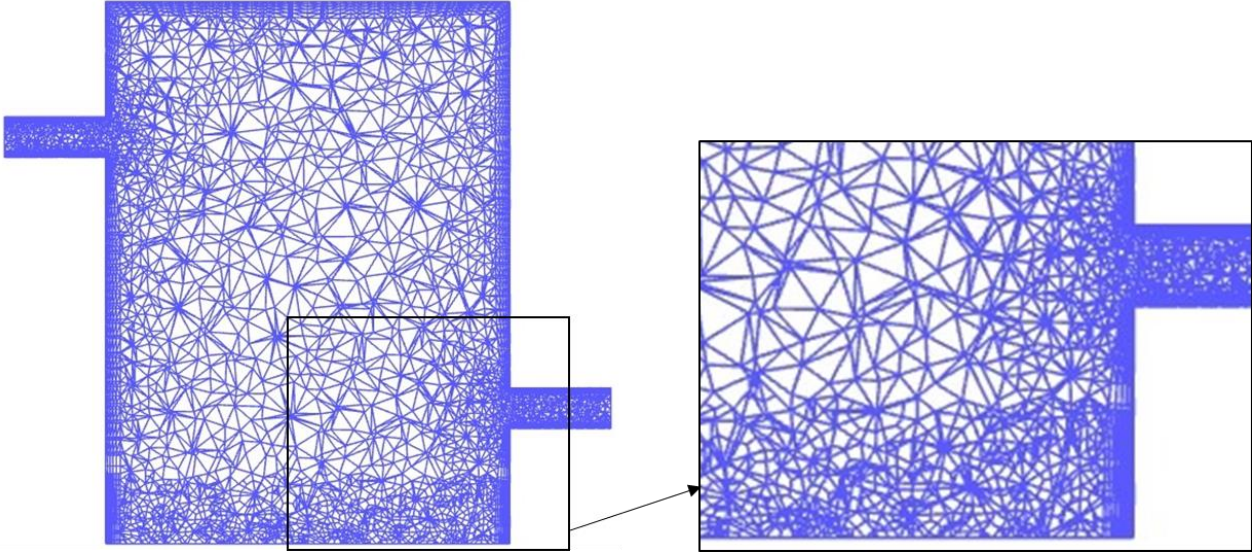

Figure 5. Plot of Mesh along the Plane of Symmetry

Task 1(b)

Task 1(a) was repeated with the same setup of simulation parameters except gravity was changed to g = -3.72 m/s^2 (strength of gravity at the surface of Mars).

Deliverable (i)

The contour plot of the y-velocity in the plane of symmetry for the steady solution is shown in Figure 6. As observed from the plot, the minimum y-velocity is -0.0505 m/s while the maximum y-velocity is 0.0342 m/s. Unlike the case in Task 1(a), the fluid flow path is different in Task 1(b). The water initially enters the inlet and travels in the positive x direction until it encounters the wall. Next, the flow direction switches to negative y direction until it encounters the bottom surface while some of the water exits the outlet pipe. The water that hits the bottom surface swings back to the left until it hits the boundary and then moves up in the positive y direction.
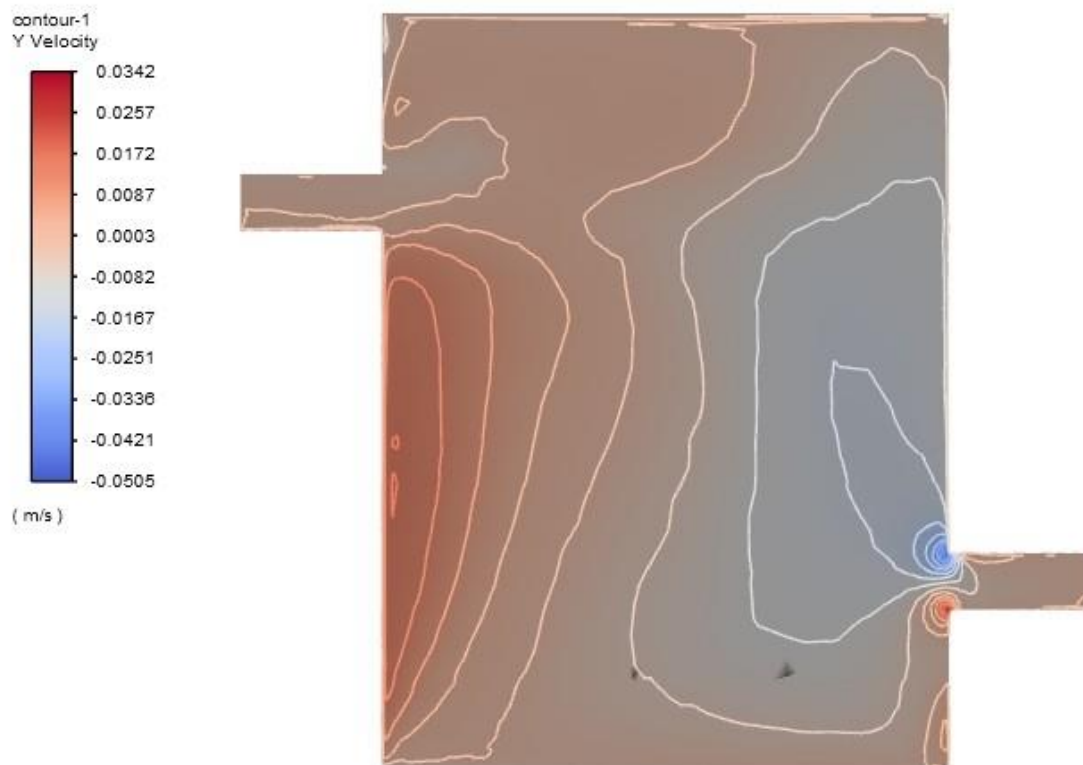

Figure 6. Contour Plot of Y-Velocity in the Plane of Symmetry

Deliverable (ii)

The contour plot of temperature in the plane of symmetry for the steady solution is shown in Figure 7. Similar to Task 1(a), the contour interval range of temperatures was manually adjusted between 293 K and 300 K to clearly highlight the "cool waterfall" feature coming from the inlet.
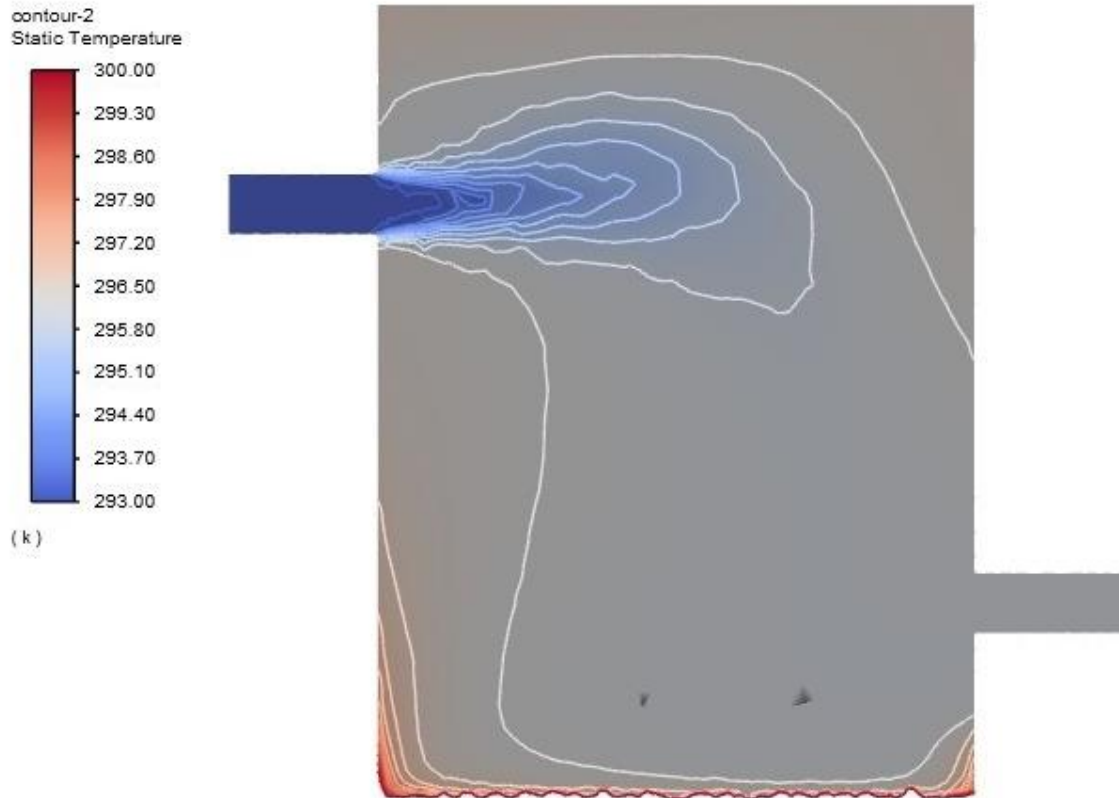

Figure 7. Contour Plot of Temperature in the Plane of Symmetry

Deliverable (iii)

The value of outlet temperature at the steady state was found to be $T_{out} = 296.31\ K$.

Figure 8 illustrates the line plot of the outlet temperature, T_{out}, as a function of the number of iterations. The convergence criteria requirement was observed between 900 and 1000 iterations where the temperature difference was 0.07 K. However, the simulation was continued to run until 1500 iterations.
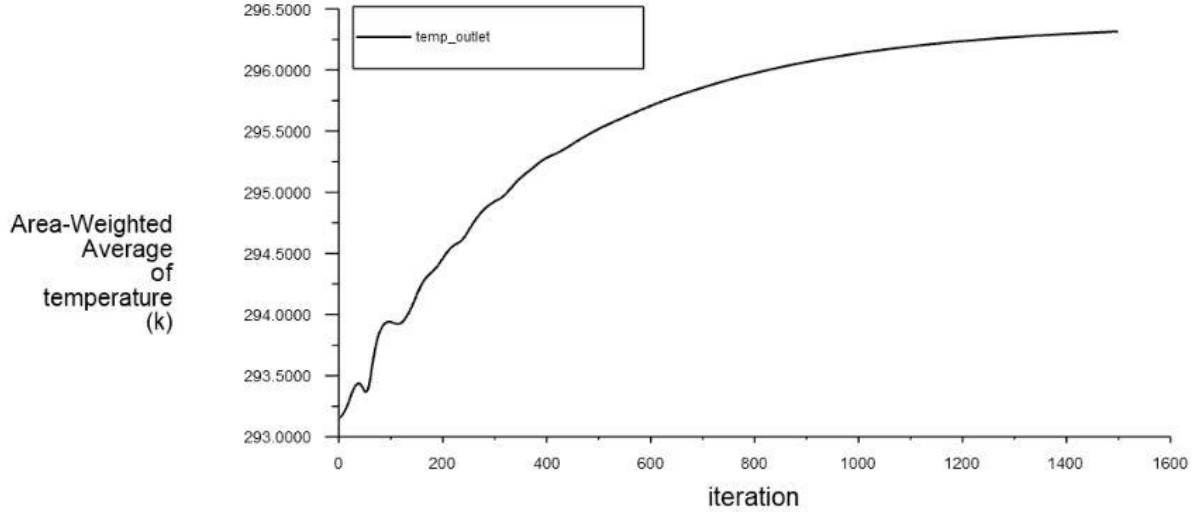
Figure 8. Line Plot of Outlet Temperature vs. Number of Iterations

Task 2

Unlike the prototype water heater design used in Task 1, a more efficient coiled pipe design as shown in Figure 9 was considered in this Task to perform simulation. The helical pipe was generated with its center traced by the equation of a helical curve:

$$X(t) = R \cos(t) \tag{5}$$

$$Y(t) = R \sin(t) \tag{6}$$

$$Z(t) = C\,t \tag{7}$$

The curve was traced from parameter t = 0 to t = 12 π (radian), with a radius R = 0.3 m and the parameter C = 0.15/(2 π) m. The cross section of the helical pipe is circular with a radius of 4 cm. For the inlet velocity, four different cases were set with v_{in} = 0.01, 0.02, 0.04, and 0.08 m/s. The inlet temperature was set to T_{in} = 300 K for all four cases. A uniform heat flux of Q = 600 W/m^2 was applied on the wall of the helical pipe and the outlet condition was set to outflow. Pressure based solver was utilized with constant density setting for the water fluid circulated through the coiled pipe. Laminar model was selected for all simulations to achieve steady state solution. The mesh was generated with an element size of 1.2 cm and program controlled inflation setting.
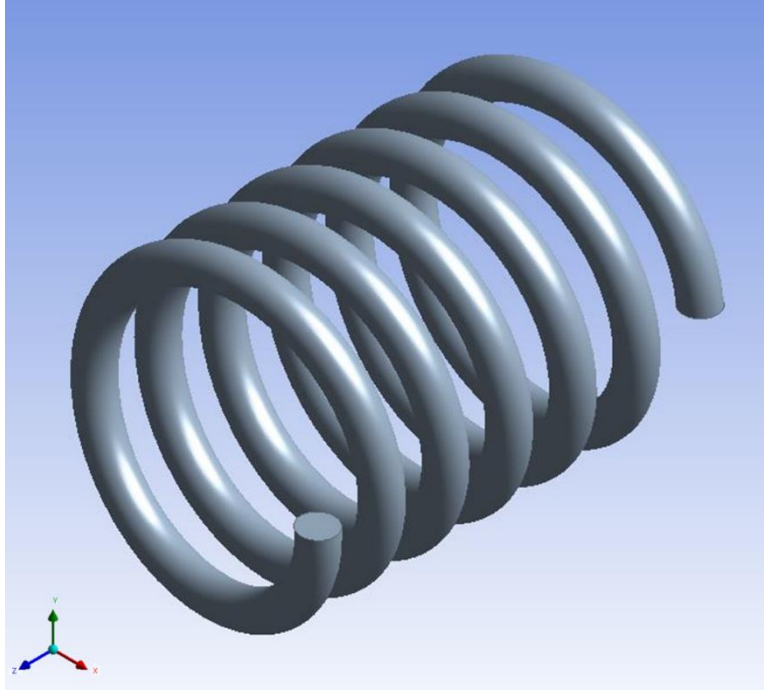
Figure 9. Coiled-Pipe Water Heater Model

Deliverable (1)

The values of temperature difference, $\Delta T = T_{out} - T_{in}$, for 4 cases of inlet velocities are shown in Table 1. The numerical values in the table are associated with those obtained from the simulations performed in Fluent while the analytical values were obtained by performing a heat budget calculation on the helical pipe system.

Eq. 8 shows the heat budget calculation for the helical water heater where $c_p = 4182$ J/kg K is the specific capacity of water, $\rho = 998.2$ kg/m^3 is the density of water, $Q = 600$ W/m^2 is the uniform heat flux applied on the pipe, and t is the transit time of the water through the pipe. A is the surface area of the helical pipe and V is the total volume of the helical pipe given by Eq. 9 and Eq. 10 respectively where $r = 4$ cm is the radius of cross section of helical pipe and L is the length of the helical pipe given by Eq. 11 defined using the parameters of helical curve, R and C stated previously.

$$c_p \, \rho \, V \, \Delta T = A \, Q \, t \tag{8}$$

$$A = 2\pi rL \tag{9}$$

$$V = \pi r^2 L \tag{10}$$

$$L = \sqrt{R^2 + C^2} \times 12\pi \tag{11}$$

In addition, the transit time of the water through the pipe can be alternately defined as shown in Eq. 12 where L is again the length of the helical pipe and v_{in} is the inlet velocity normal to the cross section of the helical pipe.

$$t = \frac{L}{v_{in}} \tag{12}$$

Substituting Eq. 9-10, 12 in Eq. 8 and simplifying, the analytical temperature difference ΔT can be computed using Eq. 13 below:

$$\Delta T = \frac{2\,Q\,L}{c_p\,\rho\,r\,v_{in}} \tag{13}$$

V_{in} (m/s)	ΔT (K) Numerical	ΔT (K) Analytical	Error %
0.01	8.76	8.19	6.96
0.02	4.47	4.10	9.02
0.04	2.28	2.05	11.22
0.08	1.15	1.02	12.74

Table 1. ΔT Values for Different Inlet Velocities

Figure 10 is a line plot of the numerical temperature difference values, ΔT, obtained by performing simulations in Fluent for 4 different cases of velocities.
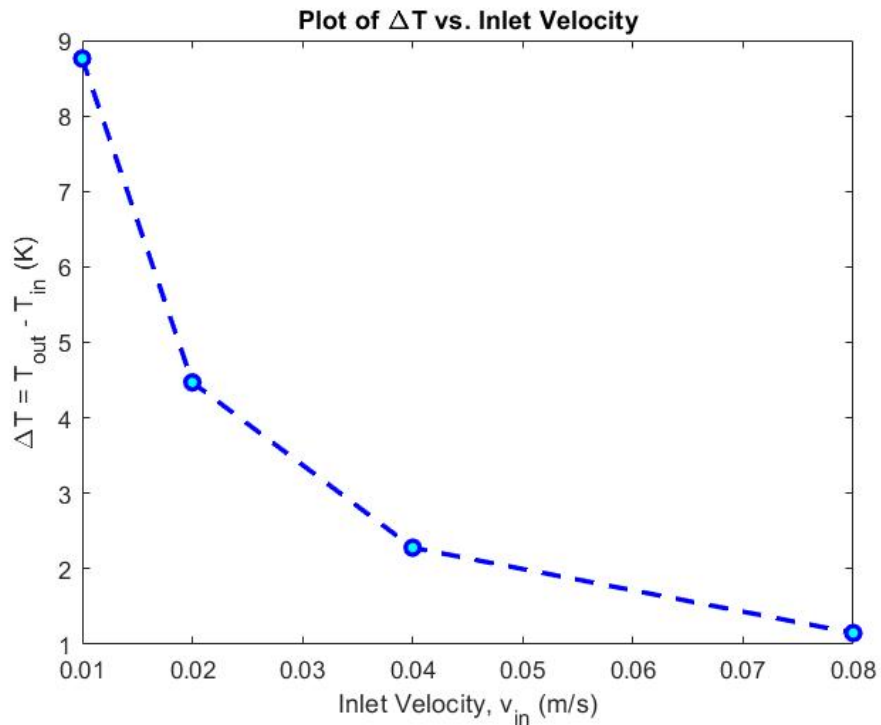

Figure 10. Plot of ΔT vs. Inlet Velocity

As observed from Figure 10, it can be discerned that the temperature difference, $\Delta T = T_{out} - T_{in}$ is inversely proportional to the inlet velocity, v_{in}. This can also be easily verified by looking at the analytical expression derived for ΔT as a function of v_{in} in Eq. 13 above. The reason behind this phenomenon is due to the fact that as the velocity of the water inside the pipe increases, the residence time decreases and the fluid does not gain enough heat from the external heat flux applied on the boundary, leading to a lower outlet temperature, T_{out} and a lower temperature difference, ΔT for a constant inlet temperature, T_{in}.

Deliverable (2)

The contour plots of temperature and velocity magnitude over the circular opening of outlet for the case with inlet velocity, $v_{in} = 0.08$ m/s are shown in Figures 11 and 12 respectively. As observed from Figure 11, the temperature at the outer edge is lower when compared to the inner edge. This can be primarily attributed to the trend of velocity magnitude at the outer and inner edges as can be seen in Figure 12, where the velocity at the outer edge is higher than the velocity at the inner edge due to the centrifugal force on the fluid as it passes through a circular path. The low velocity water at the inner edge has more residence time to gain heat from the boundary, leading to a higher temperature as explained previously.
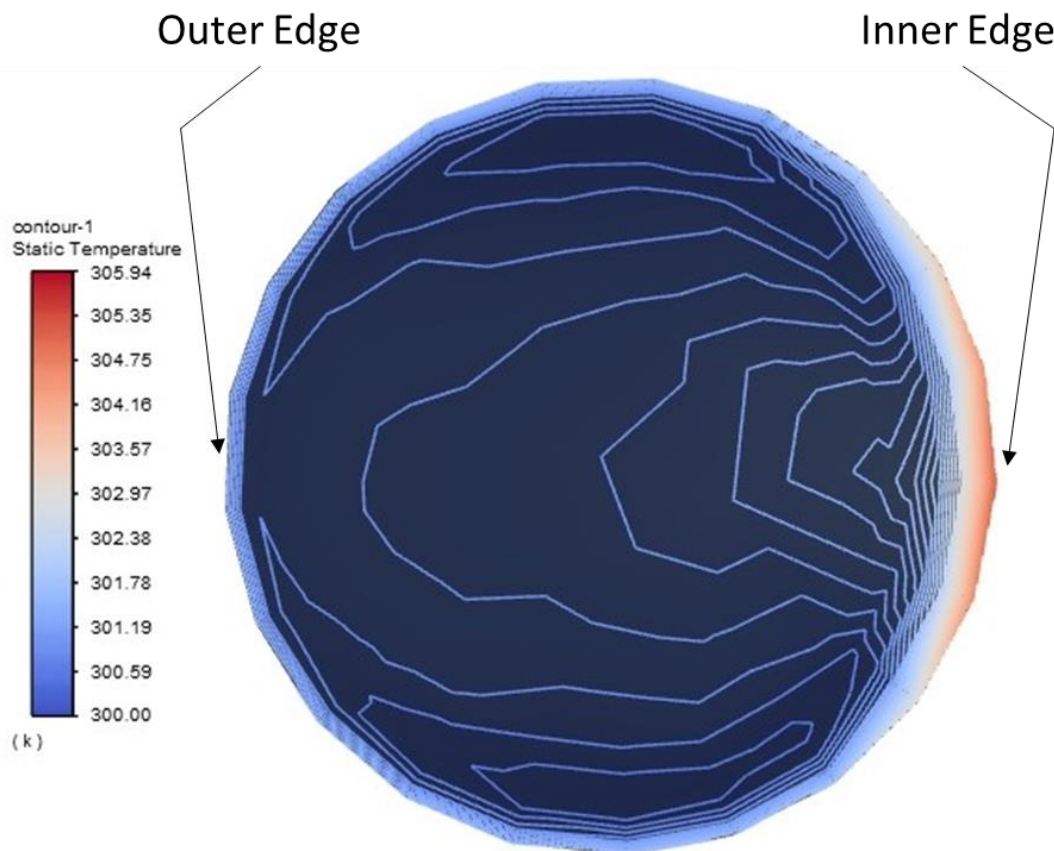

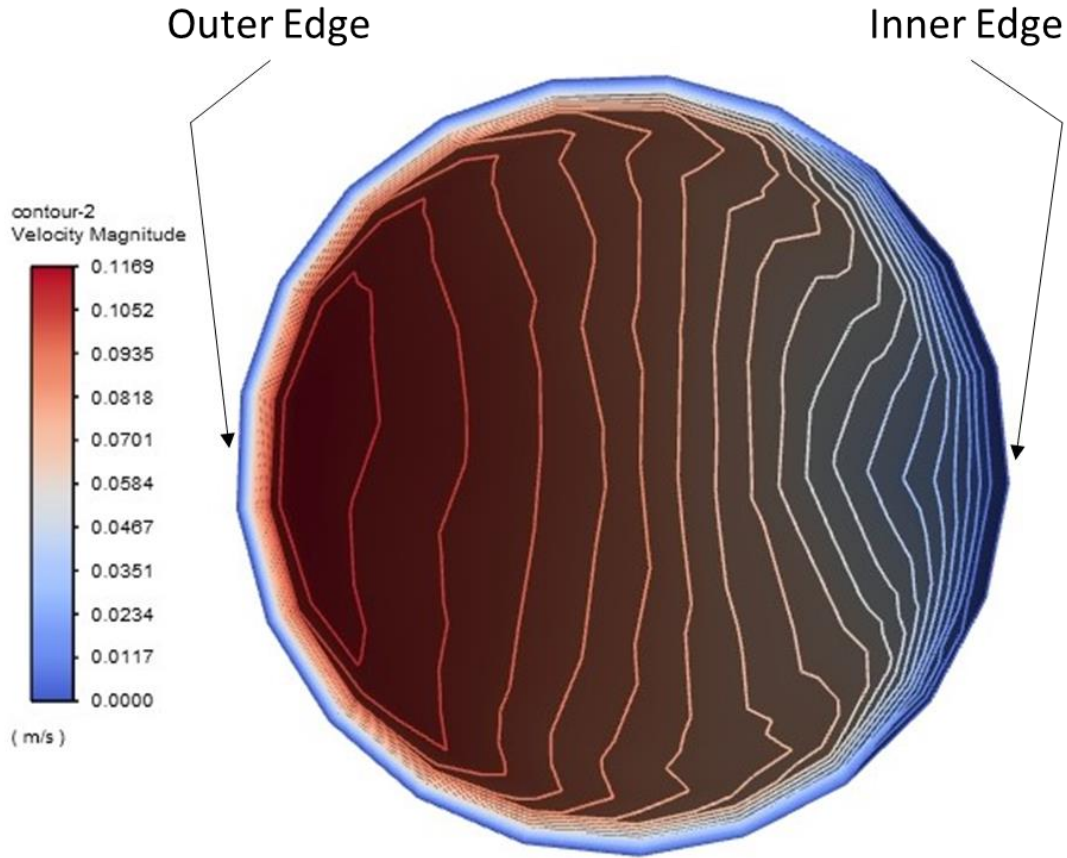Figure 11. Contour Plot of Temperature over Outlet Surface

Figure 12. Contour Plot of Velocity Magnitude over Outlet Surface

Task 3

In this task, transient simulation is performed with air as the working fluid inside the cylindrical chamber system shown in Figure 13. The main cylinder has a height of 15 cm and diameter of 30 cm, while the cylindrical side pipe has a length of 10 cm and a diameter of 5 cm located at the midplane of the main cylinder. After modeling the geometry, the mesh was generated with an element size of 1 cm. Additional mesh refinement was done by defining pancake regions of 3 cm diameter cylinders at the top and bottom portions of the main cylinder as shown in Figure 14. Since the effect of volumetric expansion is important for this case, density-based solver with ideal gas density variation setting and laminar flow is used for performing simulations. A uniform energy input of 100 W/m^2 was applied at the top and bottom plates of the main cylinder. The outlet velocity, V_{out}, is defined as the area-weighted average of velocity at outlet as shown in Eq. 14:

$$V_{out} = \frac{1}{A} \iint_A v \, dA \qquad (14)$$

where v is the outward velocity in the normal direction to the opening of the side pipe, and A is the surface area of the opening.
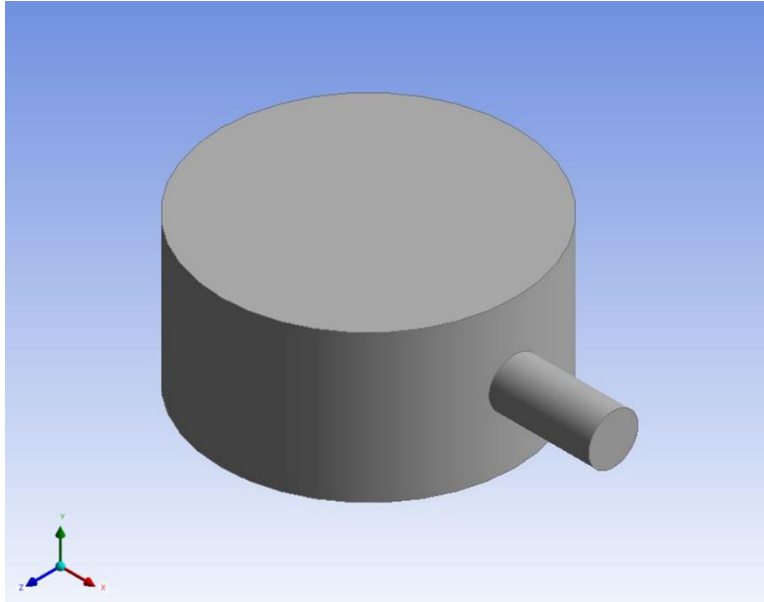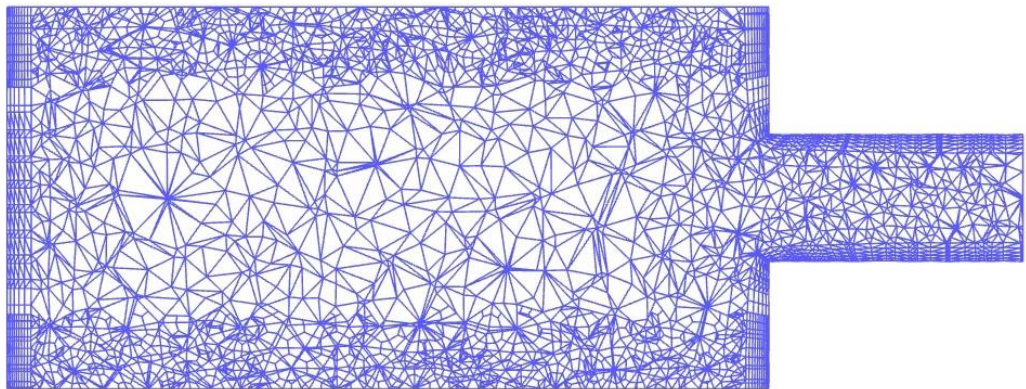
Figure 13. Heater Chamber Model

Figure 14. Plot of Mesh along the Plane of Symmetry

Deliverable (i)

The line plot of V_{out} vs. time from t = 0 to t = 5 seconds is shown in Figure 15. In this transient simulation run, the time step size was chosen as $\Delta t = 0.1$ s. Initially a trial run was done for larger time step sizes starting from 1 s to 0.5 s. However, these simulations did not result in a smooth enough plot for V_{out} vs. time. Therefore, the time step size of 0.1 s was deemed to be appropriate for the purpose of this simulation as it resulted in a smooth curve shown in the below figure. The number of time steps was set to 50 in order to achieve the solution until t = 5 s. The maximum iterations per time step was selected as 50 to allow a total of 2500 maximum number of iterations for the entire simulation run. The outlet velocity after t = 5 s was found to be $V_{out} = 0.017$ m/s.
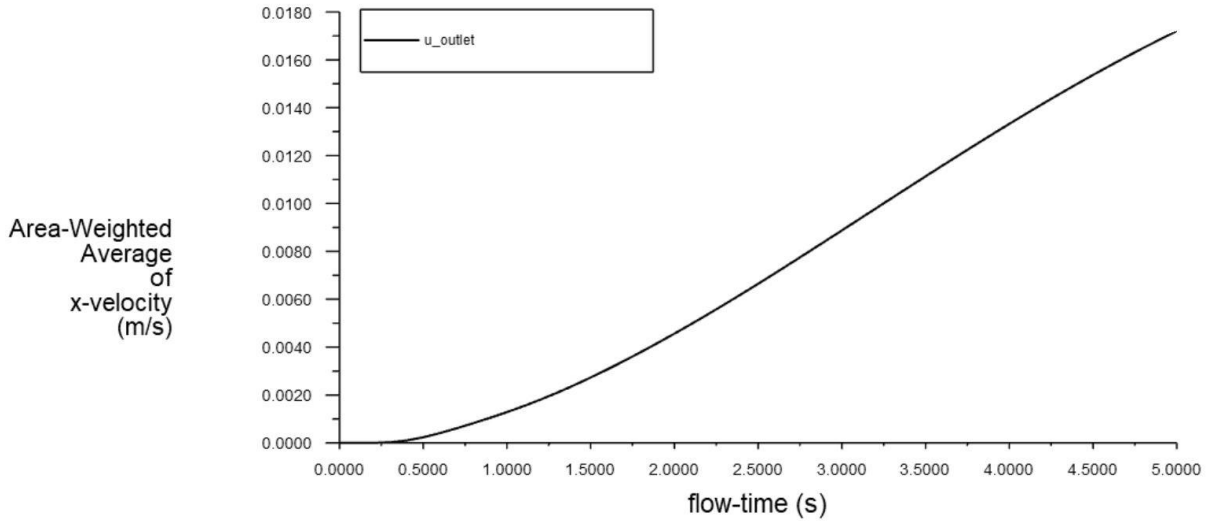
Figure 15. Line Plot of Outlet Velocity vs. Number of Iterations

Deliverable (ii)

The contour plots of pressure, temperature, density, and velocity component in the direction parallel to the side pipe, on the vertical plane of symmetry are shown in Figures 16, 17, 18, and 19 respectively. Since the air inside the cylindrical chamber is assumed to follow the ideal gas equation, the contour plots shown below are consistent with the ideal gas behavior. As the uniform heat flux is applied at the top and bottom plates, a higher temperature is observed near the end plates and a gradual decrease in temperature towards the center. Since the density follows an inverse relationship with temperature for an ideal gas, the density of the air is higher at the top and bottom plates while lower in other areas of the chamber. As the air undergoes volumetric expansion, the pressure increases inside the chamber with a gradually decreasing pressure towards the outlet. This pressure gradient allows the air to flow outside through the outlet which is consistent with the high velocity achieved towards the outer pipe region as shown in Figure 19.
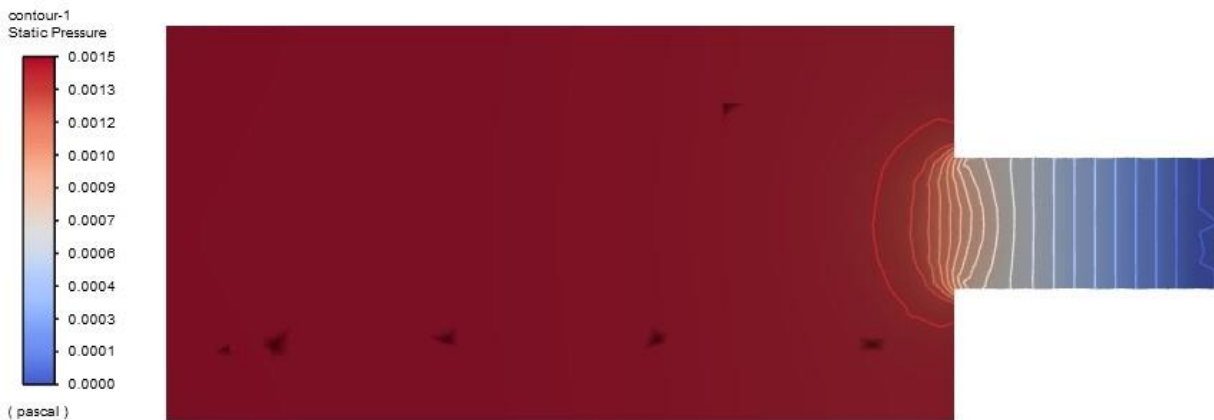

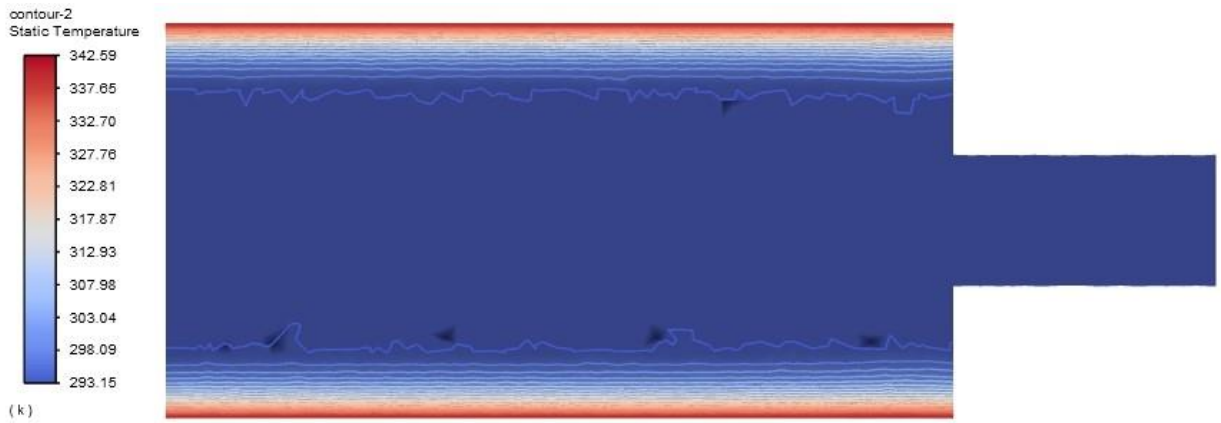Figure 16. Contour Plot of Pressure on the Vertical Plane of Symmetry

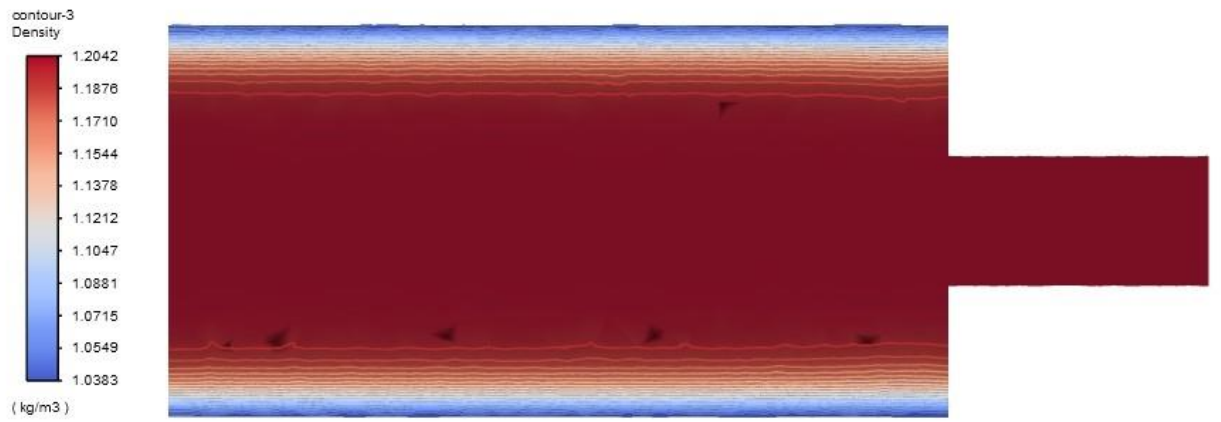Figure 17. Contour Plot of Temperature on the Vertical Plane of Symmetry

Figure 18. Contour Plot of Density on the Vertical Plane of Symmetry

Figure 19. Contour Plot of Velocity on the Vertical Plane of Symmetry

Deliverable (iii)

The fractional variation of density across the system is defined by the expression given in Eq. 15:

$$Fractional\ Variation\ of\ Density = \frac{\rho_{max} - \rho_{min}}{\bar{\rho}} \qquad (15)$$

where ρ_{max} and ρ_{min} are the maximum and minimum densities in the domain while $\bar{\rho}$ is the density averaged over the whole domain. For the system in Task 3, the maximum and minimum density values after t = 5 s can be inferred from the contour plot of density shown in Figure 16. The $\bar{\rho}$ was approximated by evaluating the volume average density over the entire domain during the simulation. Using the values of ρ_{max} = 1.2042 kg/m^3, ρ_{min} = 1.0383 kg/m^3, and $\bar{\rho}$ = 1.1821 kg/m^3, the fractional variation of density at t = 5 s for the system in Task 3 is computed to be **0.1403**.

To compare this quantity with its counterpart in Task 1, the fractional variation of density was estimated for the system in Task 1. Since the Boussinesq approximation was utilized in Task 1, the density can be estimated as a function of temperature. Substituting T_{min} = 20°C and T_{max} = 55°C in place of T_o in Eq. 2, the maximum and minimum densities in the domain are estimated to be ρ_{max} = 998.2032 kg/m^3 and ρ_{min} = 985.6035 kg/m^3. Similar to the case in Task 3, $\bar{\rho}$ was approximated by evaluating the volume average density over the entire domain during the simulation for Task 1, $\bar{\rho}$ = 993.1449 kg/m^3, which was the same value as operating density. Using these values, the fractional variation of density for the system in Task 1 was approximated to be **0.0127**. Alternately, the fractional variation of density for Task 1 can also be estimated by multiplying the thermal expansion coefficient β computed in Eq. 3 with the total temperature difference, $\Delta T = T_{max} - T_{min}$ = 35°C. The fractional variation found using this alternate method is 0.0128, which is very close to the value computed previously.

In comparison of the fractional variation of density across the systems in Task 1 and 3, the value obtained in Task 3 is much higher than that of Task 1. The main reason behind this is the fluid in system for Task 3 is considered as air following an ideal gas behavior with a volumetric expansion, where the density is a strong function of temperature. However, for the system of Task 1, the fluid considered for analysis was water, allowing the variation of density with temperature and the effect of buoyancy. In this case, the density is not a strong function of temperature, as it is evident from Eq. 2. Therefore, the fractional variation of density is found to be much lower in the case of Task 1 when compared to the system in Task 3.

Task 4

For this task, the same setup of simulation parameters used in Task 3 was repeated except running the simulation on only a quarter of the original geometry as shown in Figure 20, by invoking two-fold symmetry using two planes of symmetry. In this case, the 'top left' quarter geometry is utilized in performing the same simulation as Task 3. The mesh was also generated with an element size of 1 cm and adapting additional mesh refinement near the top region of the geometry as previously done in Task 3.
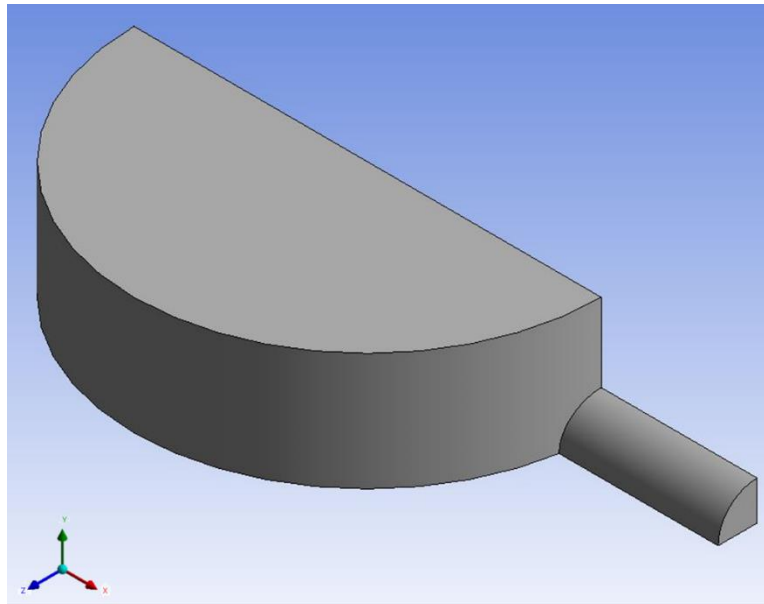

Figure 20. Quarter Geometry of Heater Chamber Model

Deliverable (i)

The line plot of V_{out} vs. time from t = 0 to t = 5 seconds is shown in Figure 21. Similar to Task 3, the time step size for this task was chosen as $\Delta t = 0.1$ s. The number of time steps was set to 50 in order to achieve the solution until t = 5 s. The maximum iterations per time step was selected as 50 to allow a total of 2500 maximum number of iterations for the entire simulation run. The outlet velocity after t = 5 s was found to be $V_{out} = 0.015$ m/s. This result is in good agreement with the value of $V_{out} = 0.017$ m/s obtained in Task 3 for the full geometry model.
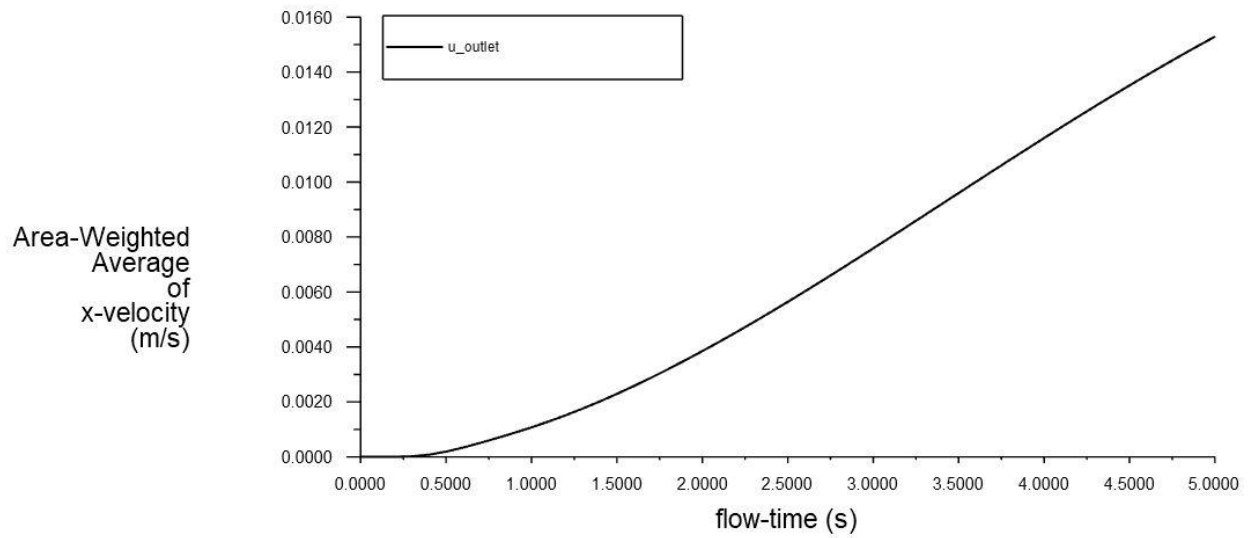
Figure 21. Line Plot of Outlet Velocity vs. Number of Iterations

Deliverable (ii)

The contour plots of temperature and velocity component in the direction parallel to the side pipe on the vertical plane of symmetry are shown in Figures 22 and 23 respectively.
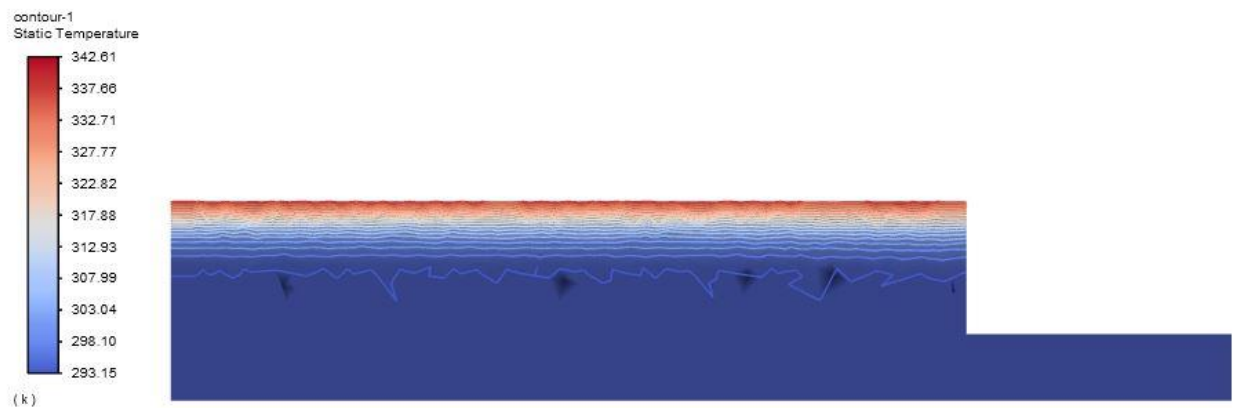

Figure 22. Contour Plot of Temperature on the Vertical Plane of Symmetry for Quarter Model

Figure 23. Contour Plot of Velocity on the Vertical Plane of Symmetry for Quarter Model

Deliverable (iii)

Figure 24 shows the plot of the mesh for the quarter geometry and Figure 25 shows the plot of the mesh along the plane of symmetry.
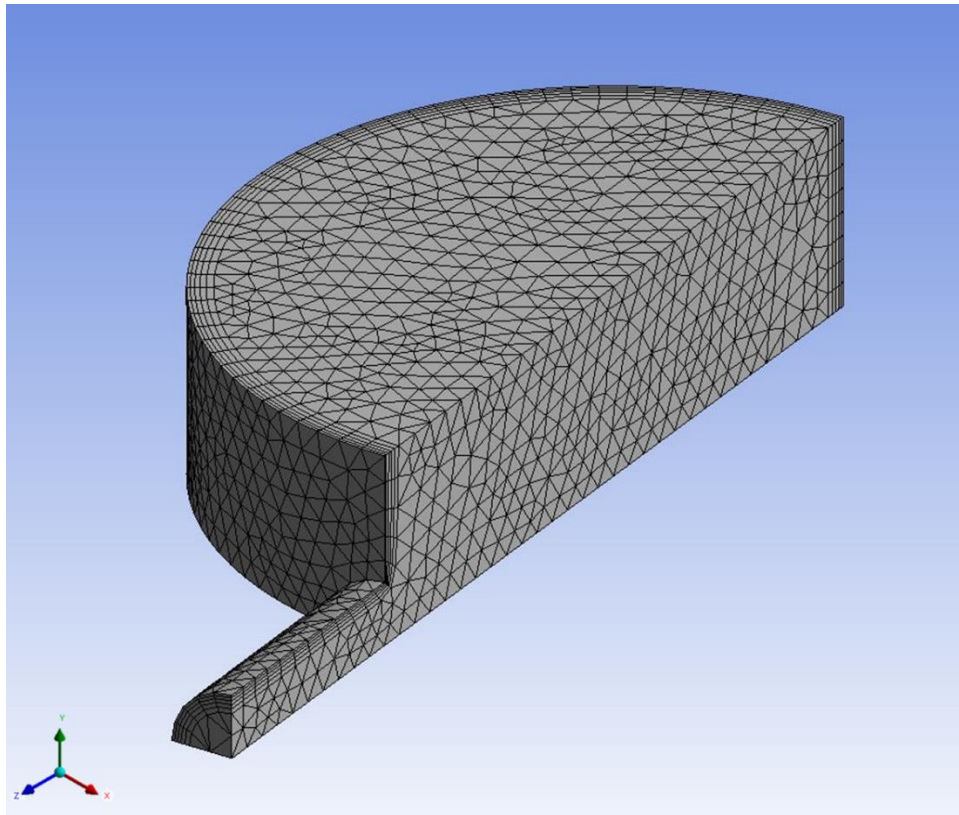

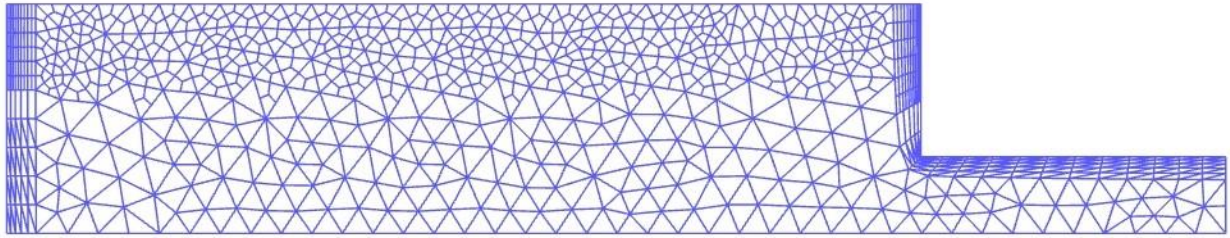Figure 24. Plot of Mesh for Quarter Model

Figure 25. Plot of Mesh along the Plane of Symmetry for Quarter Model

Deliverable (iv)

Comparing the results obtained in Task 4 and Task 3, it can be discerned that there are minor discrepancies between the values from the two tasks. The value of V_{out} obtained in Task 3 was 0.017 m/s considering the full geometry while the value of V_{out} in Task 4 was 0.015 m/s for a quarter of the full geometry, translating to approximately 11% error between the two values. Similarly, the error between the maximum temperature on the vertical plane of symmetry in Task 3 and 4 is around 5% and the error between the maximum value of x-velocity on the plane of symmetry is found to be approximately 10%.

Table 2 summarizes the savings attained by adopting the two-fold symmetry in terms of the number of elements and computational time between the two models.

Variable	Full Model	Quarter Model	% Reduction
Number of Elements	64,012	20,851	67 %
Computational Time	1733.35 seconds	535.82 seconds	69 %

Table 2. Comparison of Elements and Computational Time between Full and Quarter Models

It is evident from the above table that there is a significant savings in both the number of elements and the computational time by employing the quarter model using the two-fold symmetry. It can also be deduced that the computational time is proportional to the number of elements as the CFD software must solve a proportional number of equations at each node of the computational domain. This philosophy is very useful in larger industries as the computational time becomes very expensive. If the error percentage between the full and reduced geometries, say for example 5 %, is deemed to be acceptable, then it is recommended to go for a reduced geometry model for analysis as the savings achieved in computational time outweighs the small error between the two models.